J|A|C|S ARTICLES

Published on Web 12/02/2010

Creation of a Type 1 Blue Copper Site within a de Novo Coiled-Coil Protein Scaffold

Daigo Shiga,[†] Daisuke Nakane,[†] Tomohiko Inomata,[†] Yasuhiro Funahashi,[†] Hideki Masuda,[†] Akihiro Kikuchi,[‡] Masayuki Oda,[§] Masanori Noda,[||] Susumu Uchiyama,[||] Kiichi Fukui,[||] Kenji Kanaori,[⊥] Kunihiko Tajima,[⊥] Yu Takano,[#] Haruki Nakamura,[#] and Toshiki Tanaka*,[†]

Department of Material Sciences, Graduate School of Engineering, Nagoya Institute of Technology, Gokiso-chou, Nagoya 466-8555, Japan, Biometal Science Laboratory, RIKEN SPring-8 Center, 1-1-1, Kouto, Sayo, Hyogo 679-5148, Japan, Department of Biomolecular Chemistry, Graduate School of Life and Environmental Sciences, Kyoto Prefectural University, 1-5, Hangi-cho, Shimogamo, Sakyo-ku, Kyoto 606-8522, Japan, Department of Biotechnology, Graduate School of Engineering, Osaka University, 2-1 Yamadaoka, Suita, Osaka 565-0871, Japan, Department of Applied Biology, Kyoto Institute of Technology, Matsugasaki, Sakyou-ku, Kyoto 606-8585, Japan, and Institute for Protein Research, Osaka University, 3-2 Yamadaoka, Suita, Osaka 565-0871, Japan

Received July 23, 2010; E-mail: ttanaka@nitech.ac.jp

Abstract: Type 1 blue copper proteins uniquely coordinate Cu^{2+} in a trigonal planar geometry, formed by three strong equatorial ligands, His, His, and Cys, in the protein. We designed a stable Cu^{2+} coordination scaffold composed of a four-stranded α-helical coiled-coil structure. Two His residues and one Cys residue were situated to form the trigonal planar geometry and to coordinate the Cu^{2+} in the hydrophobic core of the scaffold. The protein bound Cu^{2+}, displayed a blue color, and exhibited UV−vis spectra with a maximum of 602−616 nm, arising from the thiolate−Cu^{2+} ligand to metal charge transfer, depending on the exogenous axial ligand, Cl^- or HPO_4^{2-}. The protein−Cu^{2+} complex also showed unresolved small $A_{||}$ values in the electron paramagnetic resonance (EPR) spectral analysis and a 328 mV (vs normal hydrogen electrode, NHE) redox potential with a fast electron reaction rate. The X-ray absorption spectrum revealed that the Cu^{2+} coordination environment was identical to that found in natural type 1 blue copper proteins. The extended X-ray absorption fine structure (EXAFS) analysis of the protein showed two typical Cu−N(His) at around 1.9−2.0 Å, Cu−S(Cys) at 2.3 Å, and a long Cu−Cl at a 2.66 Å, which are also characteristic of the natural type 1 blue copper proteins.

Introduction

Creation of a protein that can adopt a designed conformation or function at will is the ultimate goal of de novo design. Cells contain a number of metalloproteins that are required for vital activities. Therefore, metalloprotein design is becoming increasingly attractive and promising, although it is quite challenging.[1−4] Copper proteins, one of the most studied metalloproteins, participate in a variety of biological functions, such as electron transfer,[5,6] catalysis of oxidase,[7,8] oxygenase[9,10] and reductase[11] activities, and oxygen transport.[12] These functions are correlated with a variety of copper coordination geometries.

The copper coordination geometries are classified into three types, types 1−3 (Figure 1).[13,14] The type 1 copper site forms the most distorted geometry and is observed in various electron transfer proteins[5,6] and multicopper enzymes.[7,8] These proteins, which are usually referred to as blue copper proteins, exhibit unique characteristics due to their unusual coordination geometries. The Cu^{2+} ion is located in a trigonal plane formed by

[†] Nagoya Institute of Technology.
[‡] RIKEN SPring-8 Center.
[§] Kyoto Prefectural University.
[||] Graduate School of Engineering, Osaka University.
[⊥] Kyoto Institute of Technology.
[#] Institute for Protein Research, Osaka University.

(1) Kaplan, J.; DeGrado, W. F. *Proc. Natl. Acad. Sci. USA.* **2004**, *101*, 11566–11570.
(2) Ghosh, D.; Pecoraro, V. *Curr. Opin. Chem. Biol.* **2005**, *9*, 97–103.
(3) Koder, R. L.; Ross Anderson, J. L.; Solomon, L. A.; Reddy, K. S.; Moser, C. C.; Dutton, P. L. *Nature* **2009**, *458*, 305–309.
(4) Lu, Y.; Yeung, N.; Sieracki, N.; Marshall, N. M. *Nature* **2009**, *460*, 855–862.
(5) Canters, G. W.; Gilardi, G. *FEBS Lett.* **1993**, *325*, 39–42.
(6) Adman, E. T. *Adv. Protein Chem.* **1991**, *42*, 145–197.
(7) Solomon, E. I.; Sundaram, U. M.; Machonkin, T. E. *Chem. Rev.* **1996**, *96*, 2563–2605.
(8) Solomon, E. I.; Chen, P.; Metz, M.; Lee, S.-K.; Palmer, A. E. *Angew. Chem., Int. Ed. Engl.* **2001**, *40*, 4570–4590.
(9) Stewart, L. C.; Klinman, J. P. *Annu. Rev. Biochem.* **1988**, *57*, 551–592.
(10) Prigge, S. T.; Mains, R. E.; Eipper, B. A.; Amzel, L. M. *Cell. Mol. Life Sci.* **2000**, *57*, 1236–1259.
(11) Zumft, W. G.; Dreusch, A.; Lochelt, S.; Cuypers, H.; Friedrich, B.; Schneider, B. *Eur. J. Biochem.* **1992**, *208*, 31–40.
(12) Magnus, K. A.; Ton-That, H.; Carpenter, J. E. *Chem. Rev.* **1994**, *94*, 727–735.
(13) Solomon, E. I.; Baldwin, M. J.; Lowery, M. D. *Chem. Rev.* **1992**, *92*, 521–542.
(14) Solomon, E. I.; Lowery, M. D.; LaCroix, L. B.; Root, D. E. *Methods Enzymol.* **1993**, *226*, 1–33.

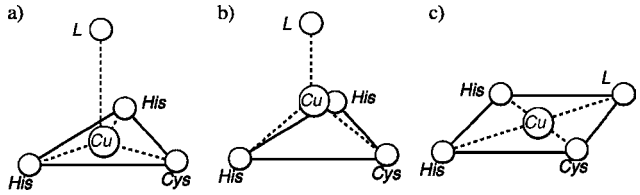

Figure 1. Structures of Cu^{2+} coordinated to His, His, Cys, and L (arbitrary). (a) Type 1: Cu^{2+} has a trigonal planar geometry and exhibits the blue color. (b) Type 1.5: Cu^{2+} has a somewhat tetrahedral geometry due to stronger axial bonding and exhibits a green color. (c) Type 2: Cu^{2+} has a square planar geometry. Type 3 consists of two copper ions linked by two oxygens and is therefore omitted in the figure. In the type 1 coordination, the Cu−S distance is short (about 2.1−2.3 Å), while the distance in type 2 is normal (2.3−2.5 Å). The Cu−N distances are normal (1.9−2.2 Å) for the both type 1 and type 2. The Cu^{2+} exists on the plane created from the His, His, Cys ligands in type 1. In type 1.5, the Cu^{2+} moves out of the plane.

three strong equatorial His, His, and Cys ligands, with one or two weakly interacting axial ligands, forming trigonal pyramidal or trigonal bipyramidal geometry. The type 1 site has intense absorptions at around 600 ($\epsilon = 2000-8000\ M^{-1}\ cm^{-1}$) and 450 nm, attributed to thiolate to Cu^{2+} ligand to metal charge transfer (LMCT).[15,16] Natural blue copper proteins have a variety of UV−vis spectral patterns. *Pseudomonas aeruginosa* azurin has a quite intense band at 628 nm ($\epsilon = 5500\ M^{-1}\ cm^{-1}$) and a weaker band at ∼450 nm and exhibits a blue color.[17] The nitrite reductase from *Alcaligenes xylosoxidans* is also blue, while those from *Achromobacter cycloclasters* and *Alcaligenes faecalis* are green, with similar, intense bands at ∼600 and ∼450 nm.[18] These proteins also have type 1 copper sites. However, in contrast to the natural proteins, the engineered blue copper sites with strong absorbance at ∼450 and ∼600 nm are often referred to as type 1.5 instead of type 1.[19]

Due to their unusual coordination geometries, type 1 copper centers are a fascinating target for de novo design. A model of the type 1 copper center has been created by substituting Cu^{2+} for Zn^{2+} in alcohol dehydrogenase, in which the catalytic Zn^{2+} is coordinated by two Cys residues, one His residue, and water in a distorted tetrahedral geometry.[20] Hellinga and Lu et al. constructed blue copper proteins, using thioredoxin and copper−zinc superoxide dismutase as native scaffolds, respectively, by protein redesign.[19,21] Schnepf et al. used a template-assembled helix bundle system.[22] However, the proteins formed the type 1.5 center, in which the copper ion moved out the trigonal plane toward the axial ligand to form a tetrahedral-like geometry (Figure 1). An insulin hexamer bound Cu^{2+} using three His, and this complex was either blue or green, depending on the thiolate compounds added to the protein as the fourth ligand.[23]

We designed a variety of metal binding sites using an α-helical coiled-coil structure as the de novo scaffold. We previously constructed a Cu^{2+} binding site with distorted geometry using His, His, and Glu residues in an α-helical coiled-coil structure.[24] In this report, by substituting the Glu residue with a Cys residue, the protein showed the representative characteristics of a type 1 blue copper protein. This work should lead not only to improvements in the design strategies of metal binding proteins but also to a better understanding of the nature of the blue copper proteins.

Results and Discussion

Design and Preparation of the Blue Copper Protein. Blue copper proteins commonly have a trigonal planar geometry, formed by the three conserved ligands, His, His, and Cys, which robustly interact with Cu^{2+}.[15] These strongly coordinating amino acid residues, His, His, and Cys, are essential for designing a blue copper protein. The Cu^{2+} configuration in the blue copper protein seems to be affected by the species of the ligand to Cu^{2+}. In particular, H_2O binding to Cu^{2+} should be avoided because it stabilizes the type 2 copper site, rather than the type 1 site. Therefore, it is essential to prevent the solvent from approaching and coordinating with the Cu^{2+}.[25] Metal−Cys complex formation usually competes with intermolecular disulfide bond formation in the presence of redox active metal ions, such as Cu^{2+}. To negate the possibilities of disulfide bond formation and solvent access to the coordinated Cu^{2+}, the most reasonable strategy would be to create a metal binding site within the hydrophobic core of the scaffold protein.

We previously constructed a distorted equatorial coordination structure of Cu^{2+} by placing His, His, and Glu residues in the hydrophobic positions of a four-helix coiled-coil protein.[24] The hydrophobic position is suitable to construct the distorted configuration of Cu^{2+} and to restrict the solvent accessibility to the Cu^{2+} ion. The Cys residue is also protected from disulfide formation when it exists within the interior of the protein. Hence, we used the four-stranded coiled-coil protein as the scaffold protein. We placed the His, His, and Cys residues to allow the Cu^{2+} to form the trigonal planar coordination geometry in the hydrophobic core of the scaffold protein, which we referred to as AM2C. The amino acid sequence of AM2C is shown in Figure 2.

To obtain the protein, the gene encoding AM2C was placed downstream of the thioredoxin gene for protein overexpression, a His-tag sequence for Ni-affinity column purification, and a thrombin site to cleave the fusion protein. From the construction of the expression plasmid, AM2C has extra G-S-A-M-A-K and R-S sequences at the N- and C-termini, respectively (Figures S1 and S2 in the Supporting Information). The fusion protein was expressed in *E. coli* BL21 (DE3), purified by Ni-affinity

(15) Messerschmidt, A.; Huber, R.; Poulos, T.; Wieghardt, K., Eds. *Handbook of metalloproteins 2*; Wiley: New York, 2001; Chapter Type-1 copper proteins, Multicopper Enzymes.
(16) Abbreviations: LMCT, metal charge transfer; RP-HPLC, reversed-phase high-performance liquid chromatography; SDS-PAGE, sodium dodecyl sulfate polyacrylamide gel electrophoresis; *C*(s), sedimentation coefficient; SV, sedimentation velocity; TCEP (tris[2-carboxyethyl]phosphine hydrochloride); PBS, phosphate-buffered saline; PIPES, piperazine-*N*,*N*′-bis(2-ethanesulfonic acid); Tris, tris(hydroxymethyl)aminomethane; ITC, isothermal titration calorimetry; K_{d}, dissociation constant; EPR, electron paramagnetic resonance; NHE, normal hydrogen electrode; XANES, X-ray absorption near edge structure; EXAFS, extended X-ray absorption fine structure.
(17) Bonander, N.; Karlsson, B. G.; Vänngard, T. *Biochemistry* **1996**, *35*, 2429–2436.
(18) Suzuki, S.; Kataoka, K.; Yamaguchi, K. *Acc. Chem. Res.* **2000**, *33*, 728–735.
(19) Hellinga, H. W. *J. Am. Chem. Soc.* **1998**, *120*, 10055–10066.
(20) Maret, W.; Dietrich, H.; Ruf, H.-H.; Zeppezauer, M. *J. Inorg. Biochem.* **1980**, *12*, 241–252.
(21) Lu, Y.; LaCroix, L. B.; Lowery, M. D.; Solomon, E. I.; Bender, C. J.; Peisach, J.; Roe, J. A.; Gralla, E. B.; Valentine, J. S. *J. Am. Chem. Soc.* **1993**, *115*, 5907–5918.
(22) Schnepf, R.; Haehnel, W.; Wieghardt, K.; Hildebrandt, P. *J. Am. Chem. Soc.* **2004**, *126*, 14389–14399.
(23) Brader, M. L.; Borchardt, D.; Dunn, M. F. *J. Am. Chem. Soc.* **1992**, *114*, 4480–4486.
(24) Shiga, D.; Nakane, D.; Inomata, T.; Masuda, H.; Oda, M.; Noda, M.; Uchiyama, S.; Fukui, K.; Takano, Y.; Nakamura, H.; Mizuno, T.; Tanaka, T. *Biopolymers* **2009**, *91*, 907–916.
(25) Daugherty, R. G.; Wasowicz, T.; Gibney, B. R.; DeRose, V. J. *Inorg. Chem.* **2002**, *41*, 2623–2638.

N-term. Q IEDKLEE ILSK**H**YA **A**ENELAR IKKLLG E**G**$_{G}$

S**G**G Q IEDKLEE ILSK**C**YA **A**ENELAR IKKLLG G**G**^{T}

G**G**K Q IEDKLEE ILSK**H**YA **A**ENELAR IKKLLG E**G**$_{G}$

C-term. Q IEDKLEE ILSK**A**YA **A**ENELAR IKKLLG G**G**^{L}

Figure 2. Amino acid sequence of AM2C. Amino acid residues in the metal binding site are indicated by underlined bold letters. Ala residues in the hydrophobic core are underlined.

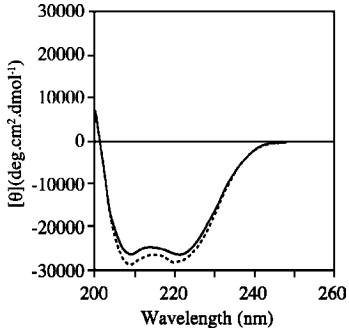

Figure 3. CD spectra of IZ-2C in the absence (solid line) and presence (dashed line) of Cu^{2+}.

column chromatography, treated with thrombin, and then subjected to RP-HPLC to purify the protein and to remove any contaminating metal ions (Figure S3 in the Supporting Information).

Protein Structural Analysis. The CD spectrum of AM2C exhibited minima at 208 and 222 nm with similar magnitudes (Figure 3). A typical coiled-coil structure has a $[\theta]_{222}$ to $[\theta]_{208}$ ratio of more than 1.[26] AM2C contains the three linkers and the extra N- and C-terminal amino acids. Hence, based on the CD spectrum, AM2C is considered to form the α-helical coiled-coil structure, even without Cu^{2+}. The CD spectrum was not affected by addition of Cu^{2+}. A nonreducing SDS-PAGE analysis revealed that the protein was monomeric, indicating that intermolecular disulfide bond formation was negligible after addition of Cu^{2+}.

The association state and size of AM2C were analyzed by analytical ultracentrifugation. The sedimentation coefficient (C(s)) distributions from sedimentation velocity (SV) experiments with 100 μM AM2C indicated that the majority of AM2C had an $s_{20,w}$ of 1.70S (Figure 4), and the estimated molecular mass of this species was 14 800 Da. This value is quite consistent with the molecular mass calculated from the amino acid sequence of AM2C (15 089 Da). In addition, the calculated $s_{20,w}$ of GCN4-pLI, based on its 3D structure (PDB ID 1GCL)[27] in the monomeric form, was 1.62S, corresponding to the observed $s_{20,w}$ of AM-2C (1.70S). These results indicate that the majority of AM2C is monomeric under these conditions. A similar result was obtained from the SV experiment with a 50 μM AM2C solution. The presence of a small amount of the dimer was also evident ($s_{20,w} = 2.5$), as shown in Figure 4. The dimer was still present under highly reducing conditions with 10 mM Tris [2-carboxyethyl] phosphine hydrochloride (TCEP), which can disrupt disulfide bond formation (Figure S4 in the Supporting Information). In addition, the dimer was not detected in a nonreducing SDS-PAGE analysis. These results show that the dimer was formed by intermolecular, noncovalent interactions. The axial dimensions (nm) of the AM2C monomer calculated from the obtained frictional ratio ($f/f_0 = 1.8$) were 30 Å × 44 Å, which agree well with the monomeric size of the four α-helical stranded coiled-coil structure.[27]

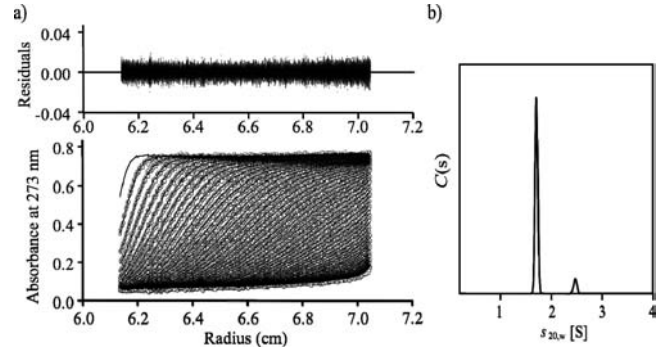

Figure 4. Analytical ultracentrifugation sedimentation data for AM-2C. (a) Sedimentation velocity (SV) experiments. The SV run of a 50 μM solution at 60 000 rpm, the results of the C(s) distribution analysis, and the residual of the fit are shown. (b) Sedimentation coefficient distribution of 100 μM AM2C from the analysis of the SV experiments.

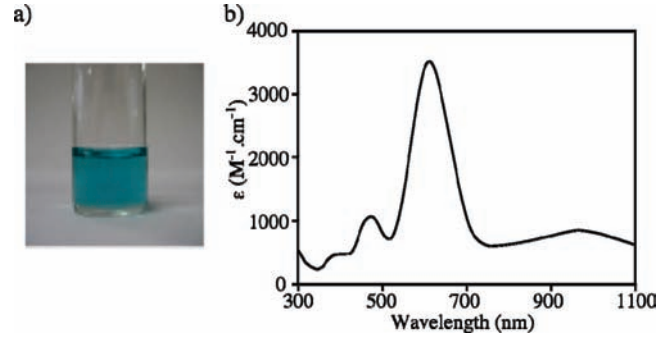

Figure 5. (a) Blue color of the solution of AM2C and Cu^{2+} in PBS. [AM2C] = 100 μM, [Cu^{2+}] = 100 μM. (b) UV−vis spectrum of AM2C−Cu^{2+} in PBS, pH 7.5. [AM2C] = 30 μM, [Cu^{2+}] = 25 μM.

UV−Vis Spectral Analysis. Addition of Cu^{2+} to the protein, each at a concentration of 100 μM, immediately turned the solution blue, which is indicative of complex formation and is characteristic of blue copper proteins (Figure 5a). Figure 5b shows the UV−vis spectrum of the AM2C−Cu^{2+} complex in phosphate-buffered saline (PBS). The AM2C−Cu^{2+} complex exhibited an intense absorption band at 616 nm and a weak band at 474 nm ($A_{474}/A_{616} = 0.30$), corresponding to S(π)−copper LMCT and S(σ)−copper LMCT, respectively.[28] A weaker band, derived from the d−d transition at 969 nm, was also observed.

When the sample was subjected to aerobic conditions, the magnitudes of the absorption bands decreased with time and the blue color faded. The color decay was a single-exponential process, with a half-life of 1.2 h (Figure S5 in the Supporting Information). On the other hand, under anaerobic conditions, the color persisted and these bands were retained. Before addition of Cu^{2+}, AM2C was sensitive to reaction with 5,5′-dithio-bis(2-nitrobenzoic acid) (DTNB, Ellman's reagent) while the color-faded protein was insensitive, indicating that the Cys residue of AM2C was oxidized. Therefore, we analyzed the

(26) Sakurai, Y.; Mizuno, T.; Hiroaki, H.; Oku, J.; Tanaka, T. *J. Peptide Res.* **2005**, *66*, 387–394.
(27) Harbury, P. B.; Zhang, T.; Kim, P. S.; Alber, T. *Science* **1993**, *262*, 1401–1407.
(28) Solomon, E. I.; Szilagyi, R. K.; George, S. D.; Basumallick, L. *Chem. Rev.* **2004**, *104*, 419–458.

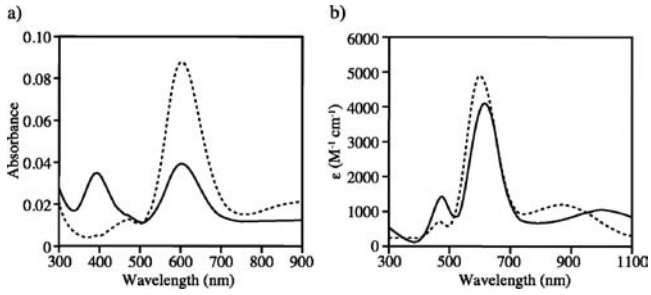

Figure 6. (a) UV−vis spectra of AM2C−Cu^{2+} in 50 mM PIPES−NaOH (solid line) and 500 mM PIPES−NaOH (dashed line). (b) UV−vis spectra of AM2C−Cu^{2+} in 20 mM PIPES−NaOH containing 500 mM NaCl (solid line) and in 500 mM KH_2PO_4 (dashed line), pH 7.5. [AM2C] = 150 μM, [Cu^{2+}] = 100 μM.

oxidation state of the Cys residue by electron spray ionization time of flight mass spectrometry (ESI-TOF MS). The mass of the protein, before addition of Cu^{2+}, was 15 088.70 Da, which is very similar to the calculated value (15 089.29 Da). On the other hand, the mass of the color-faded sample was 15 120.86 Da (Figure S6 in the Supporting Information). The molecular mass of the color-faded sample was increased by 32, indicating that the sulfur of the Cys residue was oxidized to SO_2.

Exogenous Ligand Binding. We designed only the trigonal plane formed by His, His, and Cys in the cavity of the scaffold, and hence, there is space for an exogenous ligand (X), such as H_2O, Cl^-, or HPO_4^{2-} from the PBS. To determine the identity of ligand X, we first measured the UV−vis spectrum in 50 mM piperazine-*N*,*N*′-bis(2-ethanesulfonic acid) (PIPES)−NaOH buffer (Figure 6a). Although the baseline of the spectrum was increased, due to the low solubility of the AM2C−Cu complex in this buffer, two intense bands with similar magnitudes were observed at 396 and 602 nm as well as a much weaker band at around 880 nm. These intense bands are characteristic of the type 2 and type 1 forms, respectively. On the other hand, a higher concentration of the PIPES−NaOH buffer (500 mM) increased the solubility of the complex, resulting in the disappearance of the band at 396 nm and the convergence to one band at 602 nm. Type 1 copper centers are usually destabilized by H_2O binding as an exogenous ligand.[18] Hence, the type 2 copper center created by the H_2O binding in the AM2C−Cu^{2+} complex was changed to the type 1 copper site by coordination of PIPES with the higher concentration of the PIPES−NaOH buffer (Figure 6a). This suggested that a 50 mM PIPES−NaOH buffer system could be used to evaluate the exogenous ligand.

We next measured the UV−vis spectrum in 50 mM PIPES−NaOH buffer, pH 7.5, containing either 500 mM NaCl or 500 mM KH_2PO_4 (Figure 6b). Under conditions with an excess of Cl^-, an intense band appeared at 616 nm (ϵ = 4100 M^{-1} cm^{-1}), with a weak band at 476 nm (A_{476}/A_{616} = 0.34). On the other hand, the presence of excess HPO_4^{2-} generated an intense band at 602 nm (ϵ = 4900 M^{-1} cm^{-1}), with a weak band at 468 nm (A_{468}/A_{602} = 0.14). In both cases, weaker bands were also observed at 992 and 873 nm, respectively. These results indicated that Cl^- and HPO_4^{2-} bound axially to AM2C−Cu^{2+} as exogenous ligands, resulting in the formation of the type 1 copper center, and thus suggested that the configuration of Cu^{2+} could be controlled by choosing the axial ligand for AM2C. The spectrum shown in Figure 5b resembles that with Cl^- rather than HPO_4^{2-}, indicating that Cl^- was mainly

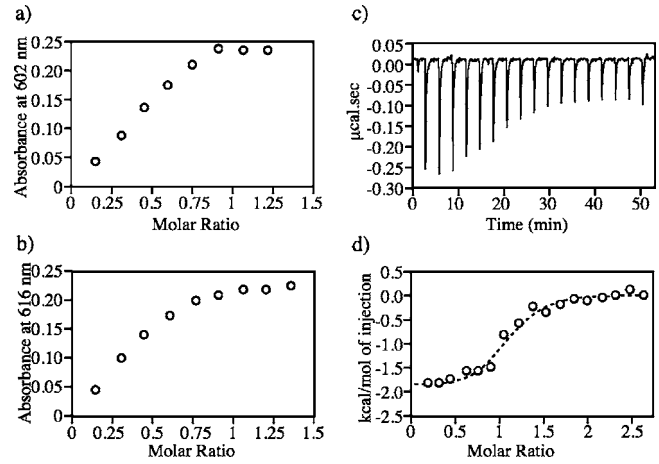

Figure 7. (Left) Titration experiment of AM2C in 50 mM PIPES containing (a) 500 mM NaCl buffer, pH 7.5 or (b) 500 mM K_2HPO_4, pH 7.5. The protein concentration was 65 μM. (Right) ITC analyses of Cu^{2+} binding to AM2C. AM2C (50 μM), in 50 mM PIPES containing 500 mM NaCl and 4 mM Tris, was added stepwise with 1.5 μL of Cu^{2+} (1 mM) in the same buffer. The raw data are shown in panel c, and the integrated area of each peak and the nonlinear, least-squares fit curve representing the heat released are shown in panel d. Each parameter was obtained as follows: $n = 1.05 \pm 0.03$, $\Delta H = -1985 \pm 80$ cal mol^{-1}, and $\Delta S = 19$ cal mol^{-1} K^{-1}.

bound to AM2C−Cu^{2+} in PBS. The axial coordination of Cl^- to Cu^{2+} was also observed in the His117Gly azurin mutant.[29]

Titration Experiment. To determine the stoichiometry between AM2C and Cu^{2+}, copper titration experiments were performed in the presence of Cl^- as the exogenous ligand. The absorption at 616 nm increased linearly with the Cu^{2+} concentration, and the change became saturated in the presence of nearly one equivalent of Cu^{2+}, suggesting 1:1 complex formation between AM2C and Cu^{2+} (Figure 7a). On the other hand, in the presence of HPO_4^{2-}, the absorption at 616 nm increased nonlinearly (Figure 7b) and never reached the theoretically maximum absorbance, which should be about 20% higher than that of the Cl^- coordinated one, as shown in Figure 5b. Addition of more Cu^{2+} resulted in the formation of a precipitate. Therefore, we did not further analyze the binding of Cu^{2+} to AM2C in the buffer containing HPO_4^{2-}.

We estimated the affinity of Cu^{2+} to AM2C in buffer containing Cl^- by an isothermal titration calorimetry (ITC) experiment. In an ITC experiment, the ligand solution should be prepared in the same buffer used to dissolve the protein. Hence, to dissolve the Cu^{2+}, Tris was added to the buffer at the lowest possible concentration to minimize its effects. The titration data fit a 1:1 stoichiometry of the protein and Cu^{2+} and generated a dissociation constant (K_d) of 2.1 μM, with a ΔH value of −1985 cal mol^{-1} and a $-T\Delta S$ value of −5662 cal mol^{-1} (Figure 7c and 7d). The metal binding process was dominated by the entropy term, which might be due to a chelation effect.[30]

Electron Paramagnetic Resonance (EPR) Spectral analysis. EPR measurements were conducted for the AM2C−Cu^{2+} complex prepared in the presence of NaCl to elucidate the coordination structure of the copper complex. The frozen solution of the copper complex exhibited a characteristic blue color similar to that before freezing (Figure 5a), suggesting that the copper

(29) den Blaauwen, T.; Canters, G. W. *J. Am. Chem. Soc.* **1993**, *115*, 1121–1129.
(30) Vallet, V.; Wahlgren, U.; Grenthe, I. *J. Am. Chem. Soc.* **2003**, *125*, 14941–14950.

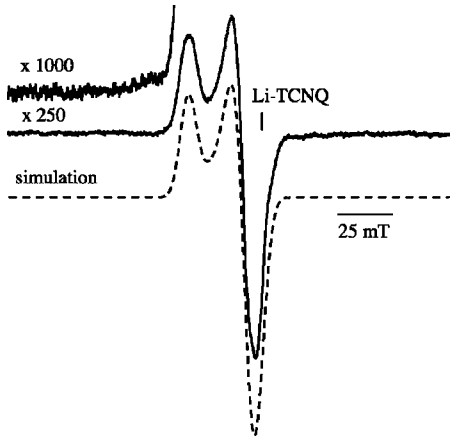

Figure 8. EPR spectrum observed for the frozen solution of the AM2C−Cu^{2+} complex at 77 K. The solution of the copper complex was prepared by the addition of Tris-HCl buffer (50 mM, pH 7.5) containing $CuCl_2$ (1.0 mM, 0.05 mL) to the AM2C solution (0.1 mM, 0.5 mL) in PIPES−NaOH buffer (50 mM, pH 7.5) containing NaCl (500 mM). The dotted line represents the simulated spectrum.

complex still retained the CT band even in the frozen matrix at 77 K. As shown in Figure 8, the observed EPR spectrum revealed the typical axial symmetric line shape ($g_{\|} = 2.255$ and $g_{\perp} = 2.064$), and no detectable EPR signals were recorded in the lower magnetic field. The AM2C−Cu^{2+} complex was proven to be the only major copper complex present in the reaction mixture. The *g* values of the complex were independent of the protein concentration (0.1 or 1 mM), indicating that the intermolecular magnetic interactions, such as the dipole or exchange interactions between the copper ions, were negligible in the present system. An analogous EPR spectrum was observed for the AM2C−Cu^{2+} complex prepared in the presence of KH_2PO_4. In contrast to the results of the optical absorption measurements (Figure 6b), the *g* values of the complex ($g_{\|} = 2.250$ and $g_{\perp} = 2.065$) agreed well with those recorded in the presence of NaCl.

Further EPR measurements were performed for the AM2C−Cu^{2+} complex to resolve the hyperfine splitting due to the copper ion ($I = 3/2$). The $g_{\|}$ component was still recorded as a broad line, even after addition of ethylene glycol (40% volume) to the solution. Second-derivative EPR measurements also failed to resolve the hyperfine splitting of the copper ion ($I = 3/2$) in the $g_{\|}$ component. In addition, the upper limit of the $A_{\|}$ value was evaluated to be ca. 15×10^{-4} cm^{-1} by means of the EPR line simulation performed for the AM2C−Cu^{2+} complex.[31]

The unusually small $A_{\|}$ value of the AM2C−Cu^{2+} complex in the EPR spectrum is a characteristic feature of the type 1 copper complex (Figure 8). Similar EPR spectra were recorded for the His117Gly mutant of *Pseudomonas aeruginosa* azurin, prepared in the presence of Cl^- ($g_{\perp}$ =2.042, $g_{\|}$ =2.340, $A_{\|} = 17 \times 10^{-4}$ cm^{-1}) and N_3^- ($g_{\perp}$ =2.041, $g_{\|}$ =2.317, $A_{\|} = 21 \times 10^{-4}$ cm^{-1}) anions as exogenous ligands,[29,32] and the coordination structure of the copper complexes was classified as the type 1 complex with a distorted trigonal plane. On the basis of the EPR results, the AM2C−Cu^{2+} complex could be classified as

(31) The EPR spectrum of the AM2C−Cu^{2+} complex was simulated by using the following parameters: $g_{\|} = 2.255$, $A_{\|} = 14 \times 10^4$ cm^{-1} (1.5 mT), line width $\delta = 6.4$ mT, $g_{\perp} = 2.064$, $A_{\perp} = 19 \times 10^4$ cm^{-1} (1.5 mT), and line width $\delta = 6.4$ mT.

(32) den Blaauwen, T.; Hoitink, C. W. G.; Canters, G. W.; Han, J.; Loehr, T. M.; Sanders-Loehr, J. *Biochemistry* **1993**, *32*, 12455–12464.

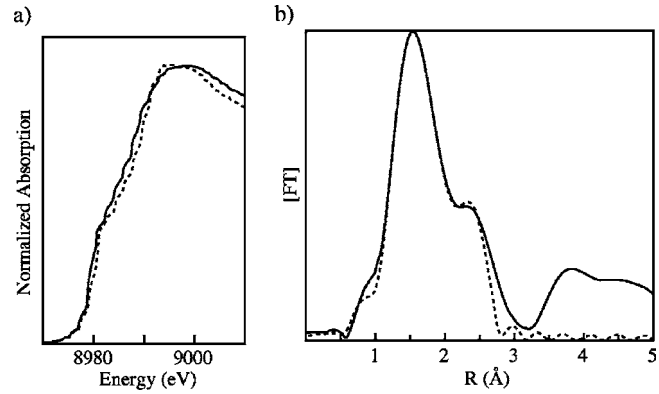

Figure 9. (a) Comparison of the normalized Cu K-edge XANES spectra of azurin (solid line) and the AM2C−Cu^{2+} complex with Cl^- as the axial ligand (dashed line). (b) FT of EXAFS of the AM2C−Cu^{2+} complex. The experimental and best-fitting curves are indicated by the solid and dashed lines, respectively.

a type 1 copper complex, in which the Cys (S) and two His (N) donors are bound to the copper ion. AM2C has five Ala residues around the metal binding site, and thus, the protein might not be tightly packed. Substitution of these Ala residues with amino acids bearing longer side chains might affect the packing of the secondary coordinate sphere, leading to a different configuration of the Cu^{2+}.

Redox Potential. The $Cu^{I/II}$ redox potential for the AM2C−Cu^{2+} complex was determined by cyclic voltammetry in PIPES−NaOH at pH 7.5 (Figure S7 in the Supporting Information). The voltammograms obtained during the multiple scans of the cyclic voltammogram, starting with the oxidized protein, reducing it, and then oxidizing it again, were identical, indicating that the $Cu^{I/II}$ redox process of AM2C−Cu^{2+} was stable. The obtained redox potential ($E_{1/2}$) was 328 mV vs NHE. Those of the natural blue copper proteins usually range from +260 to +800 mV but sometimes are over 1000 mV vs NHE.[32] For example, cucumber stellacyanin, *Pseudomonas aeruginosa* azurin, and poplar plastocyanin have redox potentials of 260, 305, and 375 mV, respectively.[33] Thus, the redox potential of AM2C−Cu^{2+} was similar to that of azurin. Furthermore, the redox process was reversible and not accompanied by structural changes. These properties of AM2C−Cu^{2+} are compatible with those of the type 1 blue copper proteins.

In general, the peak separation of the redox wave (ΔE_p) is one of the indices for the reversibility of its redox process.[34] The ΔE_p value is ca. 60 mV for the one-electron reversible redox process. In the case of the AM2C−Cu^{2+} complex, almost the same ΔE_p value (63 mV) was obtained, regardless of the various scan rates, and its anodic peak current (I_{pa}) was similar to its cathodic one (I_{pc}), suggesting that the redox process of AM2C−Cu^{2+} is reversible. These results indicate that the AM2C−Cu^{2+} complex does not undergo a structural change during its $Cu^{I/II}$ redox process.

X-ray Absorption Spectroscopy. The general spectral shape of the X-ray absorption near-edge structure (XANES) of the AM2C−Cu^{2+} complex bound with Cl^- is quite similar to that of the oxidized azurin from *Pseudomonas* sp. (Sigma, MO, USA) (Figure 9a). Although the coordination environment

(33) Li, H.; Webb, S. P.; Ivanic, J.; Jensen, J. H. *J. Am. Chem. Soc.* **2004**, *126*, 8010–8019.

(34) Bard, A. J.; Faulkner, L. R. *Electrochemical Methods: Fundamentals and Applications*, 2nd ed.; Wiley: New York, 2001.

Table 1. EXAFS Analysis of the AM2C−Cu^{2+} Complex[a]

	N^b	r (Å)	σ^2 (Å^2)	ΔE_0 (eV)
Cu−N(His)	1	1.93	0.002	6.9
Cu−N(His)	1	1.98	0.002	6.9
Cu−S(Cys)	1	2.30	0.01	7.2
Cu−Cl	1	2.66	0.002	7.1

[a] The coordination numbers (N), distances (r), Debye−-Waller factors (σ^2), and energy shifts (ΔE_0) are shown. These parameters were obtained from the EXAFS data by the fitting procedure over the r range of 1.1−2.7 Å. The residual of the fit, which was defined as $\Sigma\{\varphi_{exp} - \varphi_{theo}\}/\Sigma\{\varphi_{exp}\} \times 100$, was 2.5%. [b] Fixed parameters for the curve-fitting procedure

of azurin (five coordinated ligands) differs from that of AM2C−Cu^{2+} (four coordinated ligands, confirmed by an extended X-ray absorption fine structure (EXAFS) analysis; vide infra), the XANES spectrum strongly suggested the presence of a type 1 copper site in AM2C in conjunction with the UV−vis and EPR spectral analyses.

The Fourier-transformed Cu K-edge k^3-weighted EXAFS function of the AM2C−Cu^{2+} complex with Cl^- is shown in Figure 9b. The curve-fitting analysis was performed by assuming the presence of a typical type 1 copper site with four coordinating ligands. The best-fit values are listed in Table 1.

X-ray crystal structural analyses of the type 1 copper proteins revealed that the Cu−S distance was about 2.1−2.3 Å, and the two Cu−N distances were 1.9−2.2 Å. The axial interactions are usually more than 2.5 Å apart.[33,35] The short Cu−S distance is one of the characteristics of the type 1 copper sites. The obtained distances calculated for AM2C−Cu^{2+} were within those reported for the natural blue copper proteins (Table 1).

Structural Modeling of AM2C. We investigated the coordination geometry of the active site in the model of the AM2C−Cu^{2+} complex, using molecular mechanics simulations. Since the crystal structure of AM2C has not been reported, the model of the AM2C−Cu^{2+} complex was constructed and minimized by using the conjugate gradient method. A superposition of the minimized structure on the starting structure is shown in Figure 10a. Overall, in spite of the distance restraints using the EXAFS data, the backbone root-mean-square deviation (rmsd) was 1.09 Å, and thus, there are few differences in the backbone structures between the minimized and starting structures.

In the active site of the model of the AM2C−Cu^{2+} complex, the Cu^{2+} ion was coordinated strongly by a Cys residue and two His residues and weakly by a Cl^- ion. The minimized active site had an almost trigonal pyramidal molecular geometry, as shown in Figure 10b. The trigonal plane, formed by the S_γ atom from the Cys residue and the N_ϵ atoms from the His residues, was tilted from the equatorial plane in AM2C by 38° (Figure 10c). Figure 10b and 10c shows that the Cu^{2+} ion was located below the trigonal plane, consistent with the absorption at 476 nm (Figure 6b). As illustrated in Figure 10c and 10d, there was a large cavity around the metal binding site, surrounded by the Ala residues of the fourth and fifth layers in AM2C, although the interior of the model of the AM2C−Cu^{2+} complex was well packed with Leu or Ile residues (Figure S8 in the Supporting Information). A Cl^- ion was present in the cavity in the minimized model of the AM2C−Cu^{2+} complex, indicating that the Cl^- ion had sufficient space for movement. Substitution of these Ala residues with amino acids bearing longer side chains might affect the ligand coordination to the Cu^{2+} ion. In particular, since the distance between the Cu^{2+} ion and the C_β atoms of the Ala residue in the fourth layer is 5.12 Å, the substituted residue is expected to be coordinated to the Cu^{2+} ion.

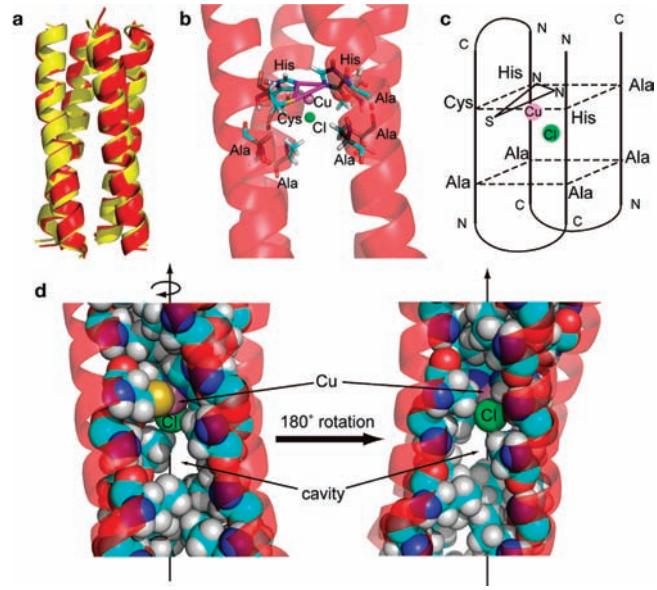

Figure 10. (a) Ribbon diagram showing the superposition of the minimized structure of the model of the AM2C−Cu^{2+} complex (red) and the starting structure (yellow). (b) Side view of the active site of the minimized structure of the model of the AM2C−Cu^{2+} complex. Pink and green spheres indicate the Cu^{2+} and Cl^- ions, respectively. The trigonal plane, formed by the S_γ atom from the Cys residue and the N_ϵ atoms from the His residues, is illustrated by magenta sticks. (c) Schematic view of the active site of the minimized structure of the model of the AM2C−Cu^{2+} complex. The fourth layer, composed of the C_α atoms of the His, Cys, His, and Ala residues, and the fifth layer, formed by the C_α atoms of the four Ala residues, are shown by the dotted lines, which are vertical against the α-helical axis. S and N indicate the S_γ atom from the Cys residue and the N_ϵ atoms from the His residues, respectively. The trigonal plane is tilted from the fourth equatorial layer by 38°. (d) Side view of the minimized model of the AM2C−Cu^{2+} complex, showing the inner packing. Internal amino acid residues are represented by spheres. The Cl^- ion exists in the cavity around the four Ala residues.

Conclusion

We designed the type 1 copper site in the hydrophobic core of a 4-helical coiled-coil protein, which is a completely different tertiary structure as compared to that of a natural protein. We placed His, His, and Cys residues for the type 1 copper site in the hydrophobic core. The resultant protein, AM2C, was predominantly monomeric and had a similar structure and size to the typical 4-helical coiled-coil structure of GCN4pLI.[27] We then evaluated the characteristics of the AM2C−Cu^{2+} complex, in terms of whether it resembles a type 1 copper protein by (1) UV−vis spectrum, (2) EPR spectroscopy, (3) redox potential, and (4) X-ray absorption spectroscopy. The AM2C−Cu^{2+} complex satisfied the four criteria for evaluation of the type 1 copper site. Therefore, we concluded that the de novo design of a type 1 blue copper protein was successful and that AM2C−Cu^{2+} is a blue copper protein. We verified the suitability of using an α-helical coiled-coil protein as a scaffold for the design of various types of metal ion geometries.

The K_d value for the AM2C−Cu^{2+} complex is extremely low, 2.1 μM, as compared to that for the azurin−Cu^{2+} complex, 25

(35) Koch, M.; Velarde, M.; Harrison, M. D.; Echt, S.; Fischer, M.; Messerschmidt, A.; Dennison, C. *J. Am. Chem. Soc.* **2005**, *127*, 158–166.

fM.[36] The affinity may be improved by amino acid substitutions. In addition, the exogenous ligand binding experiments suggested the presence of a cavity around the axial position of the coordinated copper ion in the AM2C−Cu^{2+} complex. The model structure generated by computer graphics also indicated the presence of a cavity around the metal binding site. These results imply that the AM2C−Cu^{2+} complex could potentially bind various inorganic ions and organic compounds, such as N_3^-, CN^-, imidazole, and organic thiolate ligands.[23,37] Such species affect the secondary coordination sphere interactions. Hence, the AM2C−Cu^{2+} complex should lead to the development of a tool to validate the correlation between the axial interacting group, the electronic structure, and the redox behavior.

Experimental Section

Buffers. PBS was composed of 10 mM phosphate buffer (pH 7.5) and 140 mM NaCl. PIPES buffer, including an anionic ligand, was prepared with PIPES and either NaCl or KH_2PO_4, dissolved in deionized water to final concentrations of 50 and 500 mM, respectively, and the pH was adjusted by addition of an NaOH solution. The buffer for the ITC experiment was prepared by adding 1 M Tris to the buffer to a final concentration of 4 mM to minimize the effect of the interaction between Cu^{2+} and Tris.

Expression and Purification Process. The gene encoding AM2C was synthesized by PCR (Supporting Information). The DNA fragment was treated with *Nco*I and *Hin*dIII and then ligated to the large *Nco*I-*Hin*dIII fragment of pET 32-S(−) with T4 DNA ligase to obtain pET32-S(−)-AM2C. AM2C was expressed in *Escherichia coli* BL21 (DE3) and purified as follows. *E. coli* cells transfected with the plasmid were cultured in LB medium (300 mL) at 37 °C. After 3 h of IPTG induction (1 mM), the cells were harvested, suspended in 50 mM phosphate buffer at pH 7.5 and 300 mM NaCl, sonicated at 0 °C, and centrifuged for 30 min at 4 °C. The supernatant was applied to a Ni-affinity column (Novagen) (4 mL). The column was washed with binding buffer (40 mL) (5 mM imidazole, 500 mM NaCl in 20 mM Tris-HCl, pH 7.9). The column buffer was then replaced by 20 mM Tris HCl, pH 8.4, containing 300 mM NaCl and 2.5 mM $CaCl_2$. Thrombin (Mochida Co.) was then added to a final concentration of 0.3 mg/mL, and the column was incubated at 4 °C overnight. The cleaved protein was eluted with binding buffer. After centrifugation, the supernatant was subjected to reversed-phase HPLC on a YMC-PACK ODS-A column (10 mm i.d. × 250 mm, 5 μm, YMC Inc., Japan) to remove impurities such as other proteins, organic compounds, and metal ions bound to AM2C. The protein was eluted with a linear gradient of CH_3CN in 0.1% TFA. The fractions containing the desired protein were collected and lyophilized. About 30 mg of protein was usually obtained from a 1 L culture. The protein solutions were prepared by dissolving the lyophilized sample into the proper buffer for each experiment.

Analytical Ultracentrifugation. Sedimentation velocity (SV) experiments were performed in buffer (20 mM sodium phosphate, 250 mM NaCl, pH 7.5) using a Proteomelab XL-I Analytical Ultracentrifuge (Beckman-Coulter, Fullerton, CA). Samples of AM2C (50 and 100 μM) were measured. Experiments were performed at 60 000 rpm and 20.0 °C using 12 mm aluminum double-sector centerpieces and a four-hole An60 Ti analytical rotor. The evolution of the resulting concentration gradient was monitored with absorbance detection optics at an appropriate wavelength (235 or 280 nm) according to the concentration of the solution, which generated an absorbance between 0.8 and 1.2. The radial increment was 0.003 cm, and at least 200 scans were collected between 6.0 and 7.25 cm from the center of the rotation axis. All SV raw data were analyzed by the continuous *C*(s) distribution model in the software program SEDFIT11.71.[38] The position of the meniscus and the frictional ratio (f/f_0) were set to vary as fitted parameters, and time-invariant (TI) noise and radian-invariant (RI) noise were removed. An additional parameter for the analysis included partial specific volumes calculated from the amino acid composition (AM2C, 0.7485 cm^3/g) and buffer density (ρ = 1.02009 g/cm^3) and viscosity (η = 1.0638 cPs) calculated using the program SEDNTERP, version 1.09. A resolution of 300 increments between 0.5 and 10 S was employed, and maximum entropy regularization was used (P = 0.68). The axial dimensions (nm) of the cylinder model (length × diameter), assuming a hydration level of 0.3 g of water/gram of protein, were estimated using the values after the sedimentation coefficients were converted to the standard conditions (water, 20 °C). The calculation of $S_{w,20}$ of AM2C, based on the 3D structure, was performed by using SOMO, implemented in the program ULTRASCAN II, version 9.68 [Brookes, E.; Demeler, B.; Rosano, C.; Rocco, M. *Eur. Biophys. J.* **2010**, *39*, 423−435.

CD Spectroscopy. CD measurements were performed on a Jasco-720 spectropolarimeter using a 2-mm cuvette at 25 °C. The protein concentrations were determined by measuring the Tyr absorbance in 6 M guanidium chloride using ϵ_{280} = 1300 M^{-1} cm^{-1} for one Tyr residue. The mean residue ellipticity, [θ], has the units of deg·cm^2·$dmol^{-1}$. CD spectra were obtained in PBS (pH 7.5) with a protein concentration of 10 μM and a metal concentration of 10 μM.

UV−Vis Spectroscopy. The measurements were obtained using a U-2800 spectrometer (HITACHI) at 25 °C. All samples were purged with N_2 gas before addition of Cu^{2+} to inhibit oxidation of the cysteine. All spectra were measured at pH 7.5.

Mass Spectrometry. Experiments were conducted by using micrOTOF-Q (Bruker Daltonics, Bremen, Germany). Typically, the solution (2 μL) was electrosprayed from gold-coated capillaries, prepared in house. The denatured peptide was prepared by adding a small amount of formic acid, which unfolds the peptide. All spectra were calibrated externally by using ES Tuning Mix (Agilent Technologies, Santa Clara) and processed with the Compass software (Bruker Daltonics).

ITC Experiment. ITC experiments were performed at 20 °C on a Microcal iTC200 calorimeter (MicroCal). The protein samples were prepared in 50 mM PIPES buffer (pH 7.5), containing 500 mM NaCl and 4 mM Tris, at a protein concentration of 50 μM. The metal solutions were prepared in the same buffer at a concentration of 1 mM. Aliquots (1.5 μL) of the metal solution were injected at 3 min intervals into the 200 μL ITC cell containing the protein. Data were analyzed using the Origin software to integrate the peak volumes and calculate the baselines, and the baselines were then visually inspected and corrected.

Electron Paramagnetic Resonance (EPR) Spectroscopy. The solution of AM2C−Cu^{2+} was prepared by mixing a Tris-HCl buffer solution (50 mM, pH 7.5) containing $CuCl_2$ (1.0 mM, 0.05 mL) and an AM2C solution (0.1 mM, 0.5 mL) in PIPES−NaOH buffer (50 mM, pH 7.5) containing NaCl (500 mM), under a helium atmosphere. The resulting blue-colored solution of the AM2C−Cu^{2+} complex was carefully frozen in liquid nitrogen for EPR measurements. A similar solution of the complex was also prepared with ethylene glycol (0.2 mL) to improve the resolution of the EPR spectrum. All EPR spectra were recorded at 77 K by an X-band ESR spectrometer (TE-300, JEOL), operating with the IPRIT data analyzing software (JEOL). This software was also employed for the EPR spectrum simulation. The EPR spectra were recorded under the following conditions: microwave power of 5.0 mW, microwave frequency of 9.191 GHz, time constants of 0.1 s, sweep time 4.0 min, ESR receiver gain of 250, and 100 kHz field modulation width of 0.40 mT. The magnetic field strength was calibrated on the basis of the hyperfine splitting of the Mn^{2+} ion (8.69 mT) doped in MgO powder. Li−TCNQ (lithium salt of tetracyanoquinodimethane, *g*

(36) Marks, J.; Pozdnyakova, I.; Guidry, J. *J. Biol. Inorg. Chem.* **2004**, *9*, 281–288.
(37) Marshall, N. M.; Garner, D. K.; Wilson, T. D.; Gao, Y.-G.; Robinson, H.; Nilges, M. J.; Lu, Y. *Nature* **2009**, *462*, 113–116.
(38) Schuck, P. *Biophys. J.* **2000**, *78*, 1606–1619.

= 2.0025) was used as the external standard for estimation of the *g* values. The EPR parameters were estimated as the mean value of three independent EPR measurements.

X-ray Absorption Spectroscopy. The protein sample (150 mg) was dissolved in 50 mM PIPES buffer (pH 7.5) containing 500 mM NaCl and then was concentrated to 1−1.2 mM using an Amicon Ultra 15 filter. The solution was mixed with the metal solution (1 mM) and then lyophilized. The sample exhibited the blue color. The Cu K-edge X-ray absorption spectroscopic study was performed on the bending magnet beamline BL01B1 at the SPring-8 synchrotron radiation facility (proposal no. 2009A1988) with a Si (111) double-crystal monochromator. Harmonic contamination was rejected using a total reflection mirror. The freeze-dried sample was pressed into a pellet and maintained at 10 K during data collection. Data were measured in fluorescence mode using an ORTEC Ge 19-element solid-state detector (SSD) equipped with a Ni filter. In the present XAS data, composed of 20 different sequential measurements for the same sample, the first and final data sets were carefully compared, but no appreciable difference was observed, indicating that the X-ray damage was negligible. All of the XAS data (20 scans) were averaged and Fourier transformed over the range of $2 < k < 10$ Å^{-1} using the WinXAS software 3.1.[39] Theoretical EXAFS functions $\chi(k)$ for curve-fitting analysis were calculated using FEFF8.4[40] based on the crystal structure of nitrite reductase (PDB ID 1NDT) with the sulfur atom in Met144 replaced by a chloride atom.

Model Construction and Minimization. The model of the AM2C−Cu^{2+} complex was constructed with Swiss-PDBViewer.[41] The modeling of AM2C was based on the crystal structure of a parallel, four-stranded coiled-coil, GCN4-PLI (PDB ID 1GCL).[27] However, AM2C consists of antiparallel coiled coils, because it is a single-chain peptide. The crystal structure of the retro GCN4 leucine zipper (PD BID 1C94)[42] was used for building the second and fourth α-helical domains. The side chains of the model were replaced according to the sequence of AM2C, using SCWRL 3.0.[43] Hydrogen atoms were added using the tplgene module of myPresto.[44] All ionizable side chains were configured in their characteristic ionized states at pH 7.0. We placed a Cu^{2+} ion at the putative metal binding site of AM2C.

The starting structure was solvated in a 35 Å sphere of 5083 TIP3P water[45] molecules from the center of mass of the model. A harmonic potential of 100 kcal mol^{-1} Å^{-2} was applied to any water molecules that moved outside the sphere. The AMBER96 force field parameters[46,47] were used for the amino acids in the model of the AM2C−Cu^{2+} complex in the simulations. The atomic charges of the amino acids were obtained from the AMBER96 database.[46,47]

Conjugate gradient minimization was performed on the starting structure by using the cosgene module of myPresto.[43] The long-range, nonbonded interactions were truncated using a 12 Å cutoff distance. The nonbonded interactions were updated every 10 steps. The root-mean-square force criterion to terminate the minimizations was 0.01 kcal mol^{-1} Å^{-2}. In the minimization, the Cu−N(His), Cu−Cl, and Cu−S(Cys) atom−atom distances were restrained within 0.1 Å deviation from the EXAFS data by a harmonic potential.

Acknowledgment. We thank Mr. Yuusuke Hamano (Nagoya Institute of Technology) for preparation of the protein and Mr. Yasushi Sakaguchi (Nihon SiberHegner K. K.) for technical support with ITC measurements. This work was supported by a Grant-in-Aid for Scientific Research(C) from the Ministry of Education, Culture, Sports, Science and Technology, Japan.

Supporting Information Available: DNA sequence of AM2C, construction of the plasmids, purification of AM2C, analytical ultracentrifugation analysis, time course of the color decay, ESI-TOF-MS, redox potential measurement, and 3D model. This material is available free of charge via the Internet at http://pubs.acs.org.

JA106263Y

(39) Ressler, T. *J. Synchrotron Radiat.* **1998**, *5*, 118–122.
(40) Ankudinov, A. L.; Ravel, B.; Rehr, J. J.; Conradson, S. D. *Phys. Rev.* **1998**, *B 58*, 7565.
(41) Guex, N.; Peitsch, M. C. *Electrophoresis* **1997**, *18*, 2714–2723.
(42) Mittl, P. R. E.; Deillon, C.; Sargent, D.; Liu, N.; Klauser, S.; Thomas, R. M.; Gutte, B.; Grütter, M. G. *Proc. Natl. Acad. Sci. U.S.A.* **2000**, *97*, 2562–2566l.
(43) Canutescu, A. A.; Shelenkov, A. A.; Dunbrack, R. L., Jr. *Protein Sci.* **2003**, *12*, 2001–2014.
(44) Fukunishi, Y.; Mikami, Y.; Nakamura, H. *J. Phys. Chem. B* **2003**, *107*, 13201–13210.
(45) Jorgensen, W. L.; Chandrasekhar, J.; Madura, J. D.; Impey, R. W.; Klein, M. L. *J. Chem. Phys.* **1983**, *79*, 926–935.
(46) Cornell, W. D.; Cieplak, P.; Bayly, C. I.; Gould, I. R.; Merz, K. M., Jr; Ferguson, D. M.; Spellmeyer, D. C.; Fox, T.; Caldwell, J. W.; Kollman, P. A. *J. Am. Chem. Soc.* **1995**, *117*, 5179–5197.
(47) Kollman, P. A.; Dixon, R.; Cornell, W.; Fox, T.; Chipot, C.; Pohorille, A. In *Computer Simulation of Biomolecular Systems*; Wilkinson, A., Weiner, P., van Gunsteren, W. F., Eds.; Elsevier: New York, 1997; Vol. 3, pp 83−96.